2017 IEEE Conference on Control Technology and Applications (CCTA)
August 27-30, 2017. Kohala Coast, Hawai'i, USA

A Lagrangian UAV Swarm Formation Suitable for Monitoring Exclusive Economic Zone and for Search and Rescue

Sandeep Ameet Kumar[1] and Jito Vanualailai[2]

Abstract— **This paper presents the velocity controllers of the simple rigid-body individuals of a 2-D Lagrangian swarm model that can take up a linear formation which could be used by unmanned aerial dynamical systems for searching large areas. The velocity controllers are derived from a Lyapunov function. The Direct method of Lyapunov guarantees the stability of the system. The velocity controllers are then applied to a swarm of unmanned aerial vehicles. Simulation results are provided to support the results obtained.**

I. Introduction

It was evident after the disappearance of Malaysia Airlines Flight MH 370 that there is no satisfactory solution for searching large areas for a particular signal or feature [1]. Similarly, the surveillance of the Exclusive Economic Zones (EEZs) of the Pacific Island Countries (PICs) is an extremely difficult and expensive exercise. This is due primarily to the vast area covered by the EEZs which is almost 20 million square kilometres in total. With neither the technological capability nor the financial resources to patrol their EEZ, the PICs are victims of daily intrusions of unauthorized marine vessels. Recognizing this major problem, PICs, with the help of Australia and New Zealand, established a regional monitoring body called the Pacific Islands Forum Fisheries Agency (FFA) in 1979, with the primary aim to monitor illegal tuna fishing. It coordinates surveillance exercises using a fleet of patrol boats owned by several PICs and long-range Marine Patrol Aircraft (MPA) owned by Australia, New Zealand, the US and France. PICs depend on Australia to provide patrol boat for maritime surveillance.

Currently, 12 PICs have 22 patrol boats donated by Australia between the years 1987 and 1997. A new Pacific Patrol Boat program was unveiled in June 2014 by Australia to replace these aging boats. The regional surveillance program by FFA oversees only occasional exercises which do not cover large areas due to the limited number and operational range of patrol boats. Even though FFA has several other initiatives that monitor daily maritime traffic and illegal fishing, the problem of illegal fishing has worsened to the extent that Palau, for instance, in January 2014, declared its EEZ a 100% marine sanctuary and banned all commercial operations from it [2]. Table 1 provides an idea of the value of the tuna industry in the Pacific and the extent of illegal fishing [3].

[1]School of Mathematical & Computing Sciences, Fiji National University, Suva, Fiji sandeep.kumar2@fnu.ac.fj

[2]School of Computing, Information & Mathematical Sciences, The University of the South Pacific, Suva, Fiji jito.vanualailai@usp.ac.fj

TABLE I

In 2012, only about 10% of US\$3.9b worth of tuna caught in the EEZs of FFA member countries went to member countries. About 9% of potential revenue was lost to unregulated fishing.

US\$3.9b	First-hand value of tuna caught in FFA member country waters in 2012.
US\$7.3b	First-hand value of tuna caught in the western and central Pacific tuna fishery in 2012.
US\$230m	Value of access fees paid by foreign fishing vessel operators for access to fish in FFA members waters in 2012.
US\$380m	Value of exports to the US, Japan, and the EU from FFA members in 2012.
US\$241m	Contribution of the tuna sector to the combined GDP of FFA members in 2011.
US\$400m	Revenue lost to illegal, unreported, and unregulated fishing in the Pacific Ocean.
16,000	Pacific Islanders employed in the tuna sector in 2012.

The Unmanned Aerial Vehicle (UAV) based technology is a feasible technology for the surveillance of an Economic Exclusive Zone effectively [4]. The primary purpose of a reusable UAV is data collection via aerial surveillance. Hence UAVs are now increasingly used for border surveillance and remote sensing, environment monitoring and aerial image processing. However, the problem of searching a large area remains.

In this paper, we present a Lagrangian swarm model that has the capability of covering large areas effectively. The swarm model is developed based on the assumption that swarming is an interplay of long-range attraction and short-range repulsion between individuals in a swarm. Attraction and repulsion functions that would be part of a Lyapunov function will be formed using artificial potentials fields (APFs) method [5], [6], [7], [8], [9]. Velocity controllers for each individual of the swarm are derived from the Lyapunov function. The Direct Method of Lyapunov is used for stability analysis [10]. It is a theoretical exposition wherein a simple rigid-body model of individuals in a swarm is extended to the kinematic equations governing the planar movement of a swarm of UAVs. The results obtained are validated through simulations.

If the controllers derived in this paper that generate linear formation are applied to dynamical systems then the dynamical systems will have the ability to search and explore large areas effectively. Thus, there would be a very good model for the surveillance of an Economic Exclusive Zone effectively and as well as for search and rescue. The remainder of the paper is organized as follows: Section II gives the description of the generic swarm model. In Section III, the velocity control laws are derived for the swarm model . Section IV elaborates on the the generation of linear formation. The velocity control laws derived in Section III are applied to unmanned aerial vehicles in Section V. In Section VI, simulation studies are presented that show the linear formation of the UAVs.

II. A Two-Dimensional Swarm Model

Consider a swarm of $n \in \mathbb{N}$ individuals that we shall treat as rigid bodies. In two-dimensional space, the positions of the individuals of the swarm can be described by their translational components and their rotational component, yaw, about the vertical axis of its body-frame reference. Let the position of the i^{th} individual at time $t \geq 0$ be $(x_i(t), y_i(t))$ with yaw angle $\psi_i = \psi_i(t)$, for all $i \in \{1,2,3,\ldots,n\}$, with $(x_i(t_0), y_i(t_0)) =: (x_{i0}, y_{i0})$ and $\psi_i(t_0) = \psi_{i0}$ as initial conditions.

Definition 2.1: The i^{th} individual is a rigid body residing in a disk with center (x_i, y_i) and radius $r_i > 0$. It is described as the set

$$B_i := \{(z_1, z_2) \in \mathbb{R}^2 : (z_1 - x_i)^2 + (z_2 - y_i)^2 \leq r_i^2\}. \quad (1)$$

Let us define the *centroid of the swarm* as

$$(x_C, y_C) := \left(\frac{1}{n} \sum_{k=1}^{n} x_k, \frac{1}{n} \sum_{k=1}^{n} y_k \right). \quad (2)$$

At $t \geq 0$, let $(\upsilon_i(t), \omega_i(t), \phi_i(t)) := (x_i'(t), y_i'(t), \psi_i'(t))$ be the instantaneous velocity of the i^{th} individual. We have thus a system of first-order ODEs for the i^{th} individual:

$$x_i'(t) = \upsilon_i(t),\ y_i'(t) = \omega_i(t),\ \psi_i'(t) = \phi_i(t), \quad (3)$$

assuming the initial conditions at $t = t_0 \geq 0$ as $x_{i0} := x_i(t_0),\ y_{i0} := y_i(t_0),\ \psi_{i0} := \psi_i(t_0)$. Suppressing t, we let $\mathbf{x}_i := (x_i, y_i, \psi_i) \in \mathbb{R}^3$, and $\mathbf{x} := (\mathbf{x}_1, \mathbf{x}_2, \mathbf{x}_3, ..., \mathbf{x}_n) \in \mathbb{R}^{3n}$ be our state vectors. Also let $\mathbf{x}_0 := \mathbf{x}(t_0) := (x_{10}, y_{10}, \psi_{10}, x_{20}, y_{20}, \psi_{20}, ..., x_{n0}, y_{n0}, \psi_{n0}) \in \mathbb{R}^{3n}$. If the instantaneous velocity (v_i, w_i, ϕ_i) has a state feedback law of the form

$$\begin{aligned} \upsilon_i(t) &:= -\mu_i f_i(\mathbf{x}(t)), \\ \omega_i(t) &:= -\varphi_i g_i(\mathbf{x}(t)), \\ \phi_i(t) &:= -\chi_i h_i(\mathbf{x}(t)), \end{aligned}$$

for $i \in \{1,2,3,\ldots,n\}$, for some scalars $\mu_i, \varphi_i, \chi_i > 0$ and some functions $f_i(\mathbf{x}(t))$, $g_i(\mathbf{x}(t))$ and $h_i(\mathbf{x}(t))$, to be constructed appropriately later, and if we define $\mathbf{g}_i(\mathbf{x}) := (-\mu_i f_i(\mathbf{x}), -\varphi_i g_i(\mathbf{x}), -\chi_i h_i(\mathbf{x})) \in \mathbb{R}^3$ and $\mathbf{G}(\mathbf{x}) := (\mathbf{g}_1(\mathbf{x}), \ldots, \mathbf{g}_n(\mathbf{x})) \in \mathbb{R}^{3n}$, then the swarm of n individuals is represented by

$$\dot{\mathbf{x}} = \mathbf{G}(\mathbf{x}),\ \ \mathbf{x}(t_0) = \mathbf{x}_0. \quad (4)$$

Definition 2.2: The target for the centroid of the swarm of $n \in \mathbb{N}$ agents is a disk with center (a, b) and radius r_τ. It is described as the set

$$\tau := \{(z_1, z_2) \in \mathbb{R}^2 : (z_1 - a)^2 + (z_2 - b)^2 \leq r_\tau^2\}. \quad (5)$$

Let ψ_{ie} be the final yaw angle of the i^{th} individual at its equilibrium point. Then the equilibrium point for the i^{th} agent is $\mathbf{x}_{ie} = (x_{ie}, y_{ie}, \psi_{ie}) \in \mathbb{R}^3$. If the system has an equilibrium point, we shall denote it by

$$\mathbf{x}_e \ := \ (\mathbf{x}_{1e}, \mathbf{x}_{2e}, \ldots, \mathbf{x}_{ne}) \in \mathbb{R}^{3n}.$$

The stability of $\mathbf{x}_e$ will be analyzed using the Direct Method of Lyapunov.

III. Velocity Controllers

Consider the configuration space of system (4) free of stationary obstacles.

A. Lyapunov Function Components

We will assume that each individual in the swarm is identical; hence $r_i = r_a\ \forall\ i \in \{1,2,3,\ldots,n\}$ where r_a is the radius of the disk in which the agent is residing.

1) Attraction to the Centroid: The attractive potential function that will ensure that the i^{th} individual is attracted towards the swarm centroid is proposed to be, for $i \in \{1,2,3,\ldots,n\}$:

$$R_i(\mathbf{x}) := \frac{1}{2}\left[(x_i - x_C)^2 + \zeta\,(y_i - y_C)^2\right]. \quad (6)$$

The control variable $\zeta \in \mathbb{R}$ determines the ratio of the minor axis (y-direction) to the major axis (x-direction) affecting the eccentricity of the swarm.

2) Target of the Swarm of $n \in \mathbb{N}$ Agents: For target attraction, the following function that measures the distance between the centroid of the swarm and the target will be used and will also be included as a component of Lyapunov function for the system:

$$T(\mathbf{x}) := \frac{1}{2}\left[(x_C - a)^2 + (y_C - b)^2\right]. \quad (7)$$

3) Inter-agent Collision Avoidance: For short-range repulsion between the i^{th} and the j^{th} individual, $j \neq i$, $i, j \in \{1,2,3,...n\}$, we consider the function

$$Q_{ij}(\mathbf{x}) := \frac{1}{2}\left[(x_i - x_j)^2 + (y_i - y_j)^2 - (2r_a)^2\right]. \quad (8)$$

4) Yaw Angle Convergence: It is desired that all yaw angles converge eventually to a common value for alignment purpose [11]. For all $j \neq i$, $i, j \in \{1,2,3,...,n\}$, consider the function

$$E_{ij}(\mathbf{x}) := \frac{1}{2}\,(\psi_i - \psi_j)^2. \quad (9)$$

B. A Lyapunov Function

Let there be real numbers $\alpha > 0$, $\gamma_i > 0$, $\xi_{ij} > 0$ and $\beta_{ij} > 0$, and define, for $i, j \in \{1,2,3,\ldots,n\}$, a Lyapunov function for system (4)

$$\begin{aligned} L(\mathbf{x}) \ &= \ \sum_{i=1}^{n} T(\mathbf{x}) \left(\gamma_i R_i(\mathbf{x}) + \sum_{\substack{j=1,\\ j\neq i}}^{n} \frac{\beta_{ij}}{Q_{ij}(\mathbf{x})} \right) \\ &\quad + \sum_{i=1}^{n} \sum_{\substack{j=1,\\ j\neq i}}^{n} \xi_{ij} T(\mathbf{x}) E_{ij} + \alpha T(\mathbf{x}). \end{aligned} \quad (10)$$

It is positive over the domain

$$D(L) \;:=\; \Big\{\mathbf{x} \in \mathbb{R}^{3n} : Q_{ij}(\mathbf{x}) > 0 \;\forall\, i,j = \{1,2,\ldots,n\}, \; i \neq j \Big\}.$$

The time-derivative of the Lyapunov function along the trajectories of system (4) is

$$\begin{aligned}
\dot{L}(\mathbf{x}) &= \alpha \dot{T}(\mathbf{x}) + \sum_{i=1}^{n} \gamma_i \Big(R_i(\mathbf{x})\dot{T}(\mathbf{x}) + \dot{R}_i(\mathbf{x})T(\mathbf{x}) \Big) \\
&\quad + \sum_{i=1}^{n} \sum_{\substack{j=1,\\ j\neq i}}^{n} \beta_{ij} \frac{\dot{T}(\mathbf{x})Q_{ij}(\mathbf{x}) - T(\mathbf{x})\dot{Q}_{ij}(\mathbf{x})}{Q_{ij}^2(\mathbf{x})} \\
&\quad + \sum_{i=1}^{n} \sum_{\substack{j=1,\\ j\neq i}}^{n} \xi_{ij} \Big(E_{ij}(\mathbf{x})\dot{T}(\mathbf{x}) + \dot{E}_{ij}(\mathbf{x})T(\mathbf{x}) \Big) \\
&= \sum_{i=1}^{n} \Big[f_i(\mathbf{x}) \cdot \dot{x}_i + g_i(\mathbf{x}) \cdot \dot{y}_i + h_i(\mathbf{x}) \cdot \dot{\psi}_i \Big] \\
&= \sum_{i=1}^{n} \left[f_i(\mathbf{x}) \cdot \upsilon_i + g_i(\mathbf{x}) \cdot w_i + h_i(\mathbf{x}) \cdot \phi_i \right]
\end{aligned}$$

where

$$\begin{aligned}
f_i(\mathbf{x}) &= \frac{1}{n} \left(\alpha + \gamma_i R_i(\mathbf{x}) + \sum_{\substack{j=1,\\ j\neq i}}^{n} \left(\frac{\beta_{ij}}{Q_{ij}(\mathbf{x})} + \xi_{ij} E_{ij} \right) \right) \\
&\quad (x_C - a) + \;\gamma_i T(\mathbf{x}) \left(x_i - x_C \right) \\
&\quad -2 \sum_{\substack{j=1,\\ j\neq i}}^{n} \beta_{ij} \frac{T(\mathbf{x})}{Q_{ij}^2(\mathbf{x})} \left(x_i - x_j \right),
\end{aligned} \tag{11}$$

$$\begin{aligned}
g_i(\mathbf{x}) &= \frac{1}{n} \left(\alpha + \gamma_i R_i(\mathbf{x}) + \sum_{\substack{j=1,\\ j\neq i}}^{n} \left(\frac{\beta_{ij}}{Q_{ij}(\mathbf{x})} + \xi_{ij} E_{ij} \right) \right) \\
&\quad (y_C - b) + \;\gamma_i \zeta T(\mathbf{x}) \left(y_i - y_C \right) \\
&\quad -2 \sum_{\substack{j=1,\\ j\neq i}}^{n} \beta_{ij} \frac{T(\mathbf{x})}{Q_{ij}^2(\mathbf{x})} \left(y_i - y_j \right)
\end{aligned} \tag{12}$$

and

$$h_i(\mathbf{x}) = 2T(\mathbf{x}) \sum_{\substack{j=1,\\ j\neq i}}^{n} \xi_{ij} \left(\psi_i - \psi_j \right). \tag{13}$$

Along a trajectory of system (4) we have

$$\dot{L}(\mathbf{x}) = \sum_{i=1}^{n} \left[f_i(\mathbf{x}) \cdot \upsilon_i + g_i(\mathbf{x}) \cdot \omega_i + h_i(\mathbf{x}) \cdot \phi_i \right].$$

Let there be scalars $\mu_i > 0$, $\varphi_i > 0$ and $\chi_i > 0$ and define the instantaneous velocity components of system (4) as

$$\upsilon_i = -\mu_i f_i(\mathbf{x}), \;\; \omega_i = -\varphi_i g_i(\mathbf{x}), \;\; \phi_i = -\chi_i h_i(\mathbf{x}). \tag{14}$$

Then

$$\begin{aligned}
\dot{L}(\mathbf{x}) &= -\sum_{i=1}^{n} \left[\mu_i {f_i}^2(\mathbf{x}) + \varphi_i {g_i}^2(\mathbf{x}) + \chi_i {h_i}^2(\mathbf{x}) \right] \\
&= -\sum_{i=1}^{n} \left[\frac{\upsilon_i^2}{\mu_i} + \frac{\omega_i^2}{\varphi_i} + \frac{\phi_i^2}{\chi_i} \right] \leq 0,
\end{aligned}$$

for all $\mathbf{x} \in D(L)$.

C. Stability Analysis

At the equilibrium point $\mathbf{x}_e$, the instantaneous velocities, υ_i, ω_i and ϕ_i, are zero because $f_i = 0$, $g_i = 0$ and $h_i = 0$. Thus, the agents assume a constant configuration or arrangement about the target. Their stationary positions therefore are components of an equilibrium point $\mathbf{x}_e$ of system (4). It is easy to see that $L(\mathbf{x}_e) = 0$, $L(\mathbf{x}) > 0 \;\forall\, \mathbf{x} \neq \mathbf{x}_e$ and $\dot{L}(\mathbf{x}) \leq 0$. Hence, we conclude that equation (10) is a Lyapunov function that guarantees the stability of system (4).

IV. Linear Formation Control

Generation of a linear formation which could be used by unmanned aerial dynamical systems for exploring large areas is one of the key pillars of this work. The linear formation is formed using the control variable ζ given in equation (6). If ζ is significantly small then it will put the individuals of the swarm in a vertical linear formation. However, if ζ is significantly large then it will put the individuals of the swarm in a horizontal linear formation.

V. Application to a Swarm of Autonomous UAVs

The UAV that will be used is a miniature sized quadrotor helicopter-type analyzed in [11].

A. Quadrotor UAV Model

Definition 5.1: The i^{th} UAV is a disk with radius l and is positioned at center (x_i, y_i). The i^{th} UAV is precisely described as the set

$$V_i = \{(z_1, z_2) \in \mathbb{R}^2 : (z_1 - x_i)^2 + (z_2 - y_i)^2 \leq l^2\}. \tag{15}$$

A quadrotor aircraft usually has a rigid cross frame [12]. The i^{th} quadrotor UAV is shown in Fig. 1. It has four arms which are typically 90 degrees apart. The length of each arm is l. Thus, the kinematic model, adopted from ref. [11], of the i^{th} quadrotor UAV with respect to its center $(x_i, y_i) \in \mathbb{R}^2$ is

$$\left.\begin{aligned}
\dot{x}_i &= \upsilon_i \cos\psi_i - \omega_i \sin\psi_i - l\Phi_i \sin\theta_i, \\
\dot{y}_i &= \upsilon_i \sin\psi_i + \omega_i \cos\psi_i + l\Phi_i \cos\theta_i, \\
\dot{\psi}_i &= \mu_i, \\
\dot{\theta}_i &= \Phi_i,
\end{aligned}\right\} \tag{16}$$

where θ_i describes its orientation with respect to the line of motion and the Earth-frame $(x_E - y_E)$ reference. The linear velocities are denoted by υ_i and ω_i along the longitudinal and lateral axes, respectively, while the rotational velocities are denoted by μ_i (time derivative of ψ_i) and Φ_i (time derivative of θ_i). The altitude and the pitch and roll angles are not considered as variables for the UAV in two-dimensional planar space. The axis along which the quadrotor moves is denoted the longitudinal axis and its perpendicular counterpart along

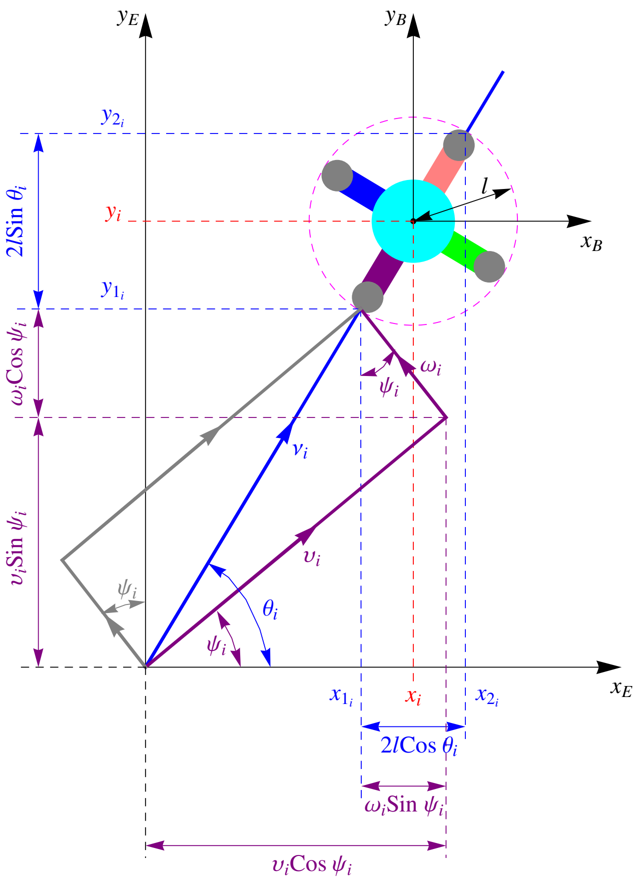

Fig. 1. Kinematic model of a Quadrotor UAV.

which it moves sideways the lateral axis. The longitudinal and lateral axes can be considered a transformation (rotation of ψ degrees) of the Body-frame reference about z_B. Thus, the i^{th} UAV is centered at (x_i, y_i), with yaw angle ψ_i. To ensure that the i^{th} UAV steers safely pass obstacles (either moving or static obstacles), we enclose the UAV by the smallest possible circle. As shown in Figure (1) the UAV is enclosed by a protective circular region centered at (x_i, y_i), with radius l. Therefore, the definition of our UAV is taken as equation (1) and the system consists of the UAVs B_i as the members of the swarm. The centroid of the swarm is given by (2) and the target of the swarm centroid is given by (5). Our aim is to design the translational velocities υ_i and ω_i and rotational velocities μ_i and Φ_i such that the UAVs are attracted to the centroid of the swarm and get into a linear formation. The centroid of the swarm is attracted to its target so that UAVs are able cover to a large area.

The Lyapunov function given by equation (10) which was derived for system (4) will be used for the system (16) with an extension to the definition of the independent variable from $\mathbf{x}_i := (x_i, y_i, \psi_i) \in \mathbb{R}^3$ to $\mathbf{x}_i := (x_i, y_i, \psi_i, \theta_i) \in \mathbb{R}^4$. Hence, the configuration vector for n vehicles become, $\mathbf{x} := (\mathbf{x}_1, \mathbf{x}_2, \mathbf{x}_3, ..., \mathbf{x}_n) \in \mathbb{R}^{4n}$ with the initial conditions vector denoted as $\mathbf{x_0} := (\mathbf{x}_1(0), \mathbf{x}_2(0), \mathbf{x}_3(0), ..., \mathbf{x}_n(0)) \in \mathbb{R}^{4n}$.

1) Equilibrium Point: Let θ_{ie} be the final orientation angle of the i^{th} vehicle at its equilibrium point. Then the equilibrium point for the i^{th} vehicle is $\mathbf{x}_{ie} = (x_{ie}, y_{ie}, \psi_{ie}, \theta_{ie}) \in \mathbb{R}^4$. If system (16) has an equilibrium point, we shall denote it by

$$\mathbf{x}_e := (\mathbf{x}_{1e}, \mathbf{x}_{2e}, \ldots, \mathbf{x}_{ne}) \in \mathbb{R}^{4n}.$$

B. Velocity Controllers of the UAVs

The system of ODEs (16) is substituted into the time derivative of (10) as shown below:

$$\begin{aligned}
\dot{L}(\mathbf{x}) &= \sum_{i=1}^{n} \left[f_i(\mathbf{x}) \cdot \dot{x}_i + g_i(\mathbf{x}) \cdot \dot{y}_i + h_i(\mathbf{x}) \cdot \dot{\psi}_i \right] \\
&= \sum_{i=1}^{n} f_i(\mathbf{x}) \left(\upsilon_i \cos\psi_i - \omega_i \sin\psi_i - l\dot{\theta}_i \sin\theta_i \right) \\
&\quad + \sum_{i=1}^{n} g_i(\mathbf{x}) \left(\upsilon_i \sin\psi_i + \omega_i \cos\psi_i + l\dot{\theta}_i \cos\theta_i \right) \\
&\quad + \sum_{i=1}^{n} h_i(\mathbf{x}) \phi_i \\
&= \sum_{i=1}^{n} \left(f_i(\mathbf{x}) \cos\psi_i + g_i(\mathbf{x}) \sin\psi_i \right) \upsilon_i \\
&\quad + \sum_{i=1}^{n} \left(g_i(\mathbf{x}) \cos\psi_i - f_i(\mathbf{x}) \sin\psi_i \right) \omega_i \\
&\quad + \sum_{i=1}^{n} \left[\left(g_i l \cos\theta_i - f_i l \sin\theta_i \right) \Phi_i + h_i(\mathbf{x}) \phi_i \right],
\end{aligned}$$

where $f_i(\mathbf{x})$, $g_i(\mathbf{x})$ and $h_i(\mathbf{x})$ are defined in (11), (12) and (13) respectively. Let there be scalars μ_i, φ_i, $\chi_i, \epsilon_i > 0$ and define the instantaneous velocity components of system (16) as

$$\begin{aligned}
\upsilon_i &:= -\mu_i \left(f_i(\mathbf{x}) \cos\psi_i + g_i(\mathbf{x}) \sin\psi_i \right), \\
\omega_i &:= -\varphi_i \left(g_i(\mathbf{x}) \cos\psi_i - f_i(\mathbf{x}) \sin\psi_i \right), \\
\Phi_i &:= -\epsilon_i \left(g_i l \cos\theta_i - f_i l \sin\theta_i \right), \\
\phi_i &:= -\chi_i h_i.
\end{aligned}$$

Then

$$\dot{L}(\mathbf{x}) = -\sum_{i=1}^{n} \left[\frac{\upsilon_i^2}{\mu_i} + \frac{\omega_i^2}{\varphi_i} + \frac{\Phi_i^2}{\epsilon_i} + \frac{\phi_i^2}{\chi_i} \right] \leq 0.$$

VI. Simulation Results for the UAV System

Simulations were generated using Wolfram Mathematica 8 software. To achieve the desired results a number of sequential Mathematica commands were executed. The positions of the obstacles were randomly generated. The target for the centroid of the swarm was also randomly generated. The arm length l of all the UAVs in all the simulations is 2.5. We numerically simulated system (16) using RK4 method (Runge-Kutta Method). At $t = 0$, the initial positions $(x_{i0}(0), y_{i0}(0))$ and orientations $\theta_i(0)$ were randomly generated.

Via numerous simulations we have shown that the UAVs from their initial positions are easily and consistently switched into a linear formation oriented perpendicular to the directions of flight as shown in Example 6.1.

Example 6.1 (**Linear Formation**): In this example, a swarm of 10 UAVs is considered. Their initial positions at time $t = 0$ are shown in Fig. 2. They cluster around the centroid as time evolves and then they move in a linear formation to their equilibrium point as a well-spaced cohesive group as shown in Fig. 3. The linear formation shown in Fig. 3 is achieved by letting the control variable $\zeta = 60$. The UAVs have the same orientation angles eventually as shown in Fig. 4 which indicates that they heading in the same direction that is $\theta_i = \theta_j$. The yaw angles converge to a common value as shown in Fig. 5 which indicates that $\psi_i = \psi_j$.

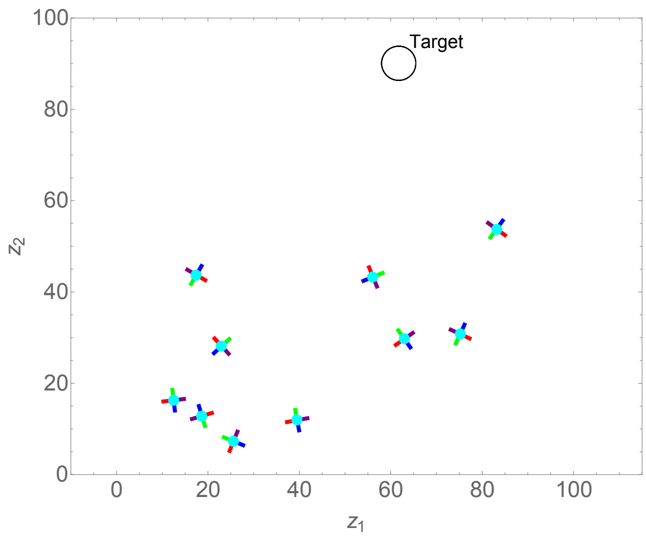

Fig. 2. ***Example 6.1***. Randomly generated initial positions and orientations of UAVs.

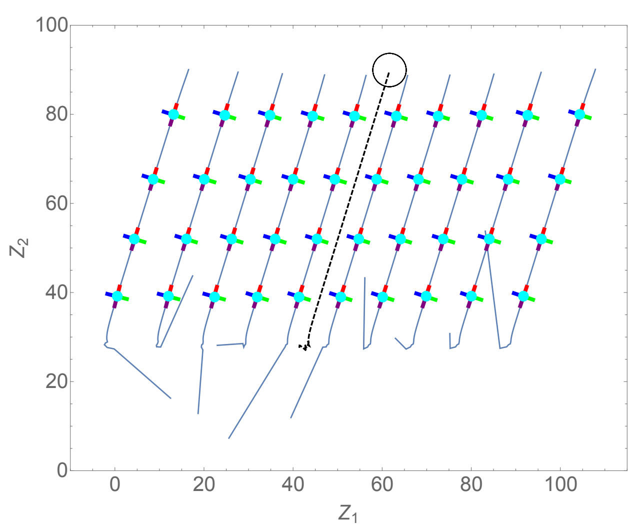

Fig. 3. ***Example 6.1***. Positions and orientations of UAVs at $t = 11, 33, 63$ and 131 respectively show the self-organization of the UAVs having a linear formation.

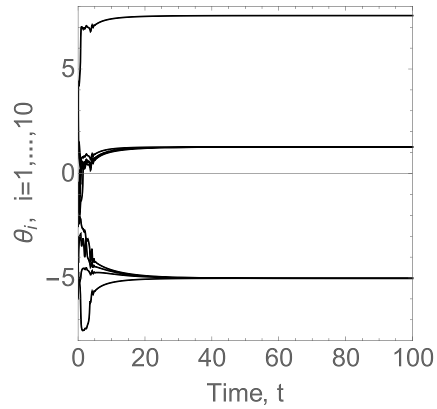

Fig. 4. ***Example 6.1***. The UAVs head in the same direction over time.

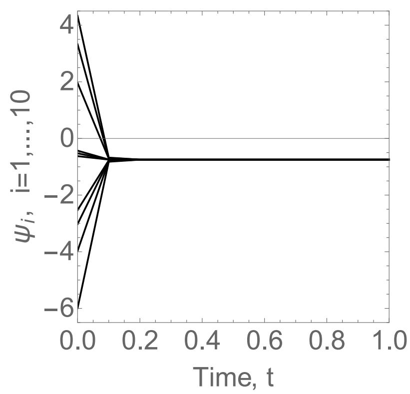

Fig. 5. ***Example 6.1***. The yaw angles converge to a common value.

VII. Conclusion

This paper presents the velocity controllers of the simple rigid-body individuals of a Lagrangian swarm model that can take up a linear formation. Via the Direct Method of Lyapunov that establishes the stability of the swarm system, we proposed the instantaneous velocity function for each individual. The velocity controllers were applied to a swarm of unmanned aerial vehicles successfully. Via computer simulations, we illustrated the linear formation. This formation could be used by unmanned aerial dynamical systems for monitoring EEZ and for search and rescue.

References

[1] J. Yang, X. Wang, and P. Bauer. Formation forming based low-complexity swarms with distributed processing for decision making and resource allocation. In *Proceedings of the 14th International Conference on Control, Automation, Robotics & Vision*, Phuket, Thailand, November 2016.

[2] Johnson, G. Palau takes fisheries surveillance to new heights: Aerial unmanned vehicles to monitor EEZ. Islands Business. November 2013.

[3] Pacific Focus Global Reach. 2013 Year in Review, The New Zealand Aid Programme, The NZ Ministry of Foreign Affairs & Trade. `http://www.aid.govt.nz/media-and-publications/publications`.

[4] R. Roy-Chaudhury. Maritime surveillance of the indian eez. *Strategic Analysis*, 22(1):49–49, 1998.

[5] O. Khatib. Real time obstacle avoidance for manipulators and mobile robots. *International Journal of Robotics Research*, 7(1):90–98, 1986.
[6] E. Rimon. Exact robot navigation using artificial potential functions. *IEEE Transactions on Robotics and Automation*, 8(5):501–517, 1992.
[7] J. Vanualailai, S. Nakagiri, and J. Ha. Collision avoidance in a two-point system via Lyapunov's second method. *Mathematics and Computers in Simulation*, 39:125–141, 1995.
[8] H. G. Tanner, S. Loizou, and K. J. Kyriakopoulos. Nonholonomic navigation and control of cooperating mobile manipulators. *IEEE Transactions on Robotics and Automation*, 19(3):53–64, 2003.
[9] C-C. Lin, C-C. Pan, and J-H. Chuang. A novel potential-based path planning of 3-d articulated robots with moving bases. *Robotica*, 22(4):359–367, 2004.
[10] A. M. Lyapunov. The general problem of the stability of motion. *International Journal of Control*, 55(3):531–773, 1992.
[11] J. Vanualailai, A. Sharan, and B. Sharma. A swarm model for planar formations of multiple autonomous unmanned aerial vehicles. In *Proceedings of the IEEE International Symposium on Intelligent Control*, August 2013.
[12] K. D. Do. Global tracking control of quadrotor vtol aircraft in three-dimensional space. *International Journal of Robotics and Automation*, 3(1):13–29, 2014.